ChemComm

COMMUNICATION

View Article Online
View Journal | View Issue

Double zipper helical assembly of deoxyoligonucleotides: mutual templating and chiral imprinting to form hybrid DNA ensembles†

Nagarjun Narayanaswamy,[a] Gorle Suresh,[b] U. Deva Priyakumar[b] and T. Govindaraju*[a]

Cite this: *Chem. Commun.*, 2015, **51**, 5493

Received 27th August 2014,
Accepted 8th September 2014

DOI: 10.1039/c4cc06759b

www.rsc.org/chemcomm

Herein, the conventional and unconventional hydrogen bonding potential of adenine in APA for double zipper helical assembly of deoxyoligonucleotides is demonstrated under ambient conditions. The quantum mechanical calculations supported the formation of hybrid DNA ensembles.

The magnificent structure–property correlations of biological systems are exemplified by the elegant molecular design and functioning of nucleic acids.[1,2] In particular, deoxyribonucleic acid (DNA) has structurally evolved over billions of years to effectively store and communicate the genetic information in majority of all living organisms.[3–5] In recent times, numerous efforts have been directed toward utilizing DNA as a potential biomaterial, a biomolecular system capable of conducting electricity, a single molecular wire and a material building block in celebrated nanotechnological advances.[6] Here, we report an adenine functionalized perylene bisimide (PBI) conjugate (**APA**) as a promising molecular template to construct hybrid DNA ensembles through double zipper helical assembly (Fig. 1). The intriguing property of adenine to form hydrogen bonds with complementary (thymine) and non-complementary (adenine and guanine) nucleobases inspired us to design **APA** as a double zipper template to construct new hybrid DNA structures.[7,8] PBI is one of the most promising aromatic π-conjugated systems with potential applications in organic electronics, biology and supramolecular architectures.[9] Recently, supramolecular architecture resulting from covalent functionalization of PBI with single-stranded (ss) DNA has been reported.[10] In this context, **APA** operates through noncovalent interactions, thus, avoiding synthetic difficulties prevalent in the covalent approaches. To the best of our knowledge, this is the first report on the construction of ordered hybrid DNA ensembles through double zipper helical assembly of deoxyoligonucleotides employing versatile hydrogen bonding and π-stacking potential of adenine in **APA**.

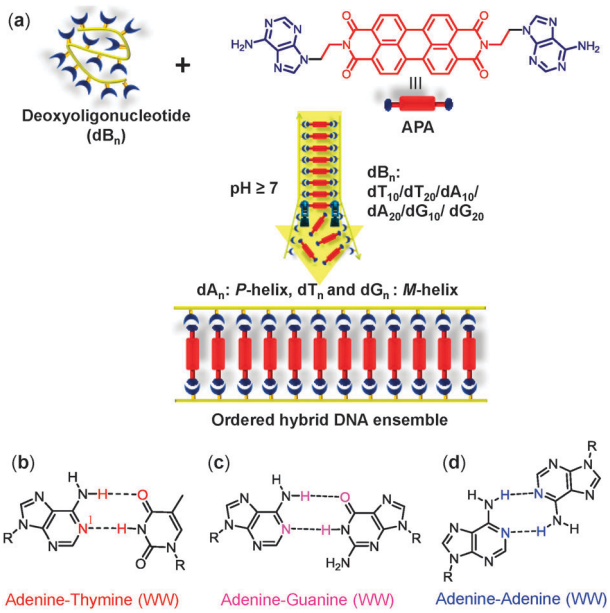

Fig. 1 (a) Molecular structure of **APA** and deoxyoligonucleotides (dB$_n$) used in the present study and schematic of hybrid DNA ensemble formation. (b–d) Hydrogen bonding in A–T, A–G and A–A base pairs. W = Watson–Crick hydrogen bonding site.

Herein, we present a new strategy for the construction of hybrid DNA ensembles of deoxyoligonucleotides (dB$_n$) employing **APA** (Fig. 1). The **APA** conjugate was prepared following our earlier reported procedure,[11] and various dB$_n$ (dA$_n$/T$_n$/G$_n$/C$_n$) were employed to construct double helical assembly of **APA** and dB$_n$ (Fig. S1, ESI†).[12] First, the molecular interactions of **APA** were studied by evaluating its photophysical properties. The UV-vis absorption spectrum of **APA** (50 μM) in DMSO exhibited three strong characteristic bands at 530,

[a] *Bioorganic Chemistry Laboratory, New Chemistry Unit, Jawaharlal Nehru Centre for Advanced Scientific Research, Jakkur P.O., Bangalore 560064, India. E-mail: tgraju@jncasr.ac.in; Fax: +91 8022082627*

[b] *Centre for Computational Natural Sciences and Bioinformatics, International Institute of Information Technology, Hyderabad 500032, India*

† Electronic supplementary information (ESI) available: Synthesis, characterization, experimental and computational procedures, UV-vis absorption, emission, CD spectra, and simulation data of **APA**–oligonucleotide hybrid ensembles. See DOI: 10.1039/c4cc06759b

493 and 461 nm corresponding to characteristic 0–0, 0–1 and 0–2 electronic transitions of the perylene chromophore, respectively.[13] The absorption spectrum of **APA** (50 μM) in aqueous solution (water/DMSO = 90 : 10, v/v%) exhibited hypsochromic shift in the 400–550 nm region and a new band at 561 nm, which is attributed to the hydrophobic force-induced aggregation of **APA** (Fig. S2a, ESI†). The fluorescence spectrum of **APA** in DMSO displayed mirror image emission bands and these bands were completely quenched in aqueous solution as a result of aggregation (Fig. S2b, ESI†).[12]

Interestingly, the absorption spectrum of **APA** (50 μM) in PBS buffer (10 mM, pH = 7, 10% DMSO) showed bathochromic shift with appreciable hypochromicity (Fig. S2a, ESI†). Next, we investigated photophysical properties of **APA** in the presence of complementary and non-complementary dB_n in PBS buffer. **APA** (50 μM) showed hyperchromicity in the absorption with increasing concentration (1–10 μM) of dB_n (Fig. S3, ESI†). These results revealed the existence of mutual interactions between **APA** and complementary as well as non-complementary dB_n through noncovalent forces to form hybrid assembly structures.

To understand the nature of molecular organizations of **APA** in the presence and absence of dB_n, we performed circular dichroism (CD) spectroscopy studies at ambient temperature (25 °C). **APA** (50 μM) gave a flat CD signal, which is ascribed to the existence of equal amounts of right- and left-handed helical aggregates. **APA** : dT_{10} (10 : 2) exhibited a bisignated CD signal in the 400–600 nm region and a negative CD signal in the 250–300 nm region corresponding to the absorption of **APA** and dT_{10}, respectively (Fig. 2a). The intense negative CD signal in the **APA** absorption region originated from the orientation of transition moments of perylene chromophores in the counter-clockwise direction (M-helix). The negative CD signal in the 250–300 nm region revealed M-helical arrangement of dT_{10} strands around the molecular template **APA**. To validate our proposed stoichiometric ratio of **APA** : dT_{10} (10 : 2), we performed concentration dependent CD measurements by titrating increasing concentrations of **APA** (0 to 70 μM) to a fixed concentration of dT_{10} (10 μM). The stoichiometry of **APA** : dT_{10} in hybrid DNA ensembles is given in terms of the base pair ratio *i.e.* A : T (A of **APA** : T of dT_{10}). The plot of CD intensity at 561 nm (perylene) against the A/T ratio showed saturation at 1 : 1 suggesting a stoichiometry of 10 : 2 for the formation of the [dT_{10} : (**APA**)$_{10}$: dT_{10}] type ensemble (Fig. 2c). We also recorded the CD spectra of fixed concentration of **APA** (50 μM) by adding increasing concentration of dT_{10} (0 to 12 μM). The plot of CD intensity monitored at 561 nm against concentration of dT_{10} showed saturation at 10 μM (Fig. S4, ESI†). Thus, CD studies confirmed a stoichiometric ratio of 10 : 2 for the complexation of **APA** and dT_{10} to form [dT_{10} : (**APA**)$_{10}$: dT_{10}] ensembles.

Next, CD spectra of **APA** in the presence of non-complementary dA_{10}, dG_{10} and dC_{10} were recorded. Notably, **APA** : dC_{10} (10 : 2) combination did not display any characteristic CD signals indicating the absence of ordered assembly between **APA** and dC_{10} (Fig. 2a). Surprisingly, **APA** : dA_{10} (10 : 2) and **APA** : dG_{10} (10 : 2) showed unprecedented P-(right handed) and M-helical arrangements with respect to both perylene chromophore (400–600 nm) and dB_n (B = A or G)

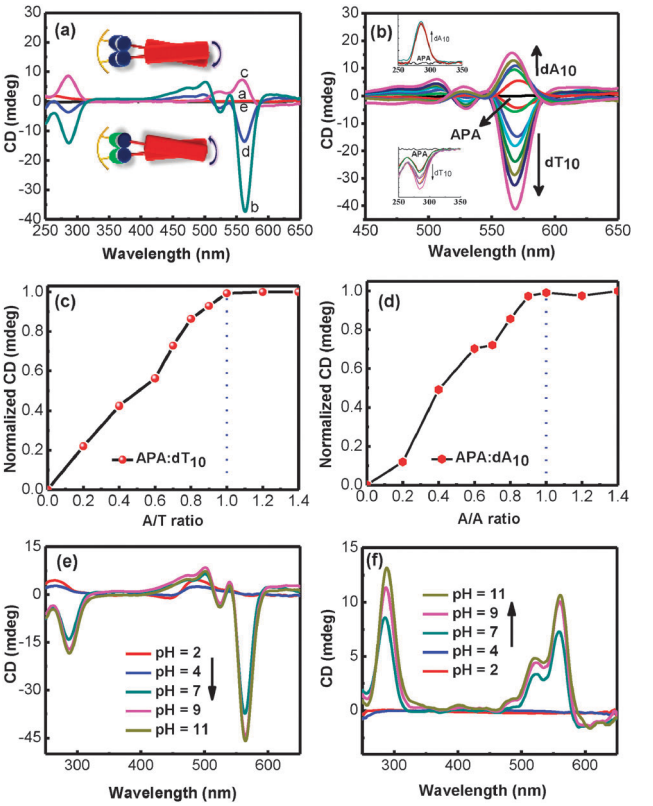

Fig. 2 CD spectra of **APA**. (a) a: **APA**, and **APA** and dB_n (10 : 2 ratio), b: dT_{10}, c: dA_{10}, d: dG_{10} and e: dC_{10} in PBS buffer (10 mM, pH = 7, 10% DMSO). Inset: right and left-handed helical orientation of **APA** in the presence of dA_{10} (top) and dT_{10}/G_{10} (bottom). (b) Spectra of **APA** with variable concentration of dA_{10} and dT_{10}. Inset: spectral features of **APA** and dA_{10} or dT_{10} in the A/T absorption region. (c) & (d) Plots of CD intensity monitored at 561 nm for **APA** and dT_{10} or dA_{10} different combinations of A/T and A/A ratios at fixed concentration of dT_{10} (10 μM) and dA_{10} (10 μM) respectively. pH dependent spectra of **APA** templated hybrid DNA ensembles of dT_{10} (e) and dA_{10} (f).

(250–300 nm) (Fig. 2a). The stoichiometry study performed with **APA** and dB_{10} (dA_{10} and dG_{10}) also suggested the formation of [dB_{10} : (**APA**)$_{10}$: dB_{10}] in the ratio of 10 : 2 (**APA** : dB_{10}) (Fig. 2d and Fig. S5, ESI†). This indicated mutual templating between **APA** and dA_{10}/dG_{10} through unconventional hydrogen bonding leading to P- and M-helical imprinting in the hybrid DNA ensembles. In the control study, spectra of individual dA_{10} showed positive and negative signals at 270 nm and 250 nm respectively (Fig. S6, ESI†). Similarly, dT_{10} showed positive and negative signals at 280 nm and 250 nm respectively. These CD signals correspond to their respective random coil structures.[12] Therefore, the characteristic features in the CD spectra of dT_{10}, dA_{10} and dG_{10} with **APA** in the nucleobase and perylene absorption regions, as discussed above, signify the formation of ordered chiral assemblies. The spectra of **APA** as a function of added dT_{10}/dA_{10} exhibited an increase in the intensity of CD signals in the perylene chromophoric region (Fig. 2b). These data suggest that the dB_n concentration drives the formation of ordered [dB_n:(**APA**)$_n$:dB_n] ensembles. Furthermore, we observed similar CD changes of **APA** with $dA_{20}/dT_{20}/dG_{20}$ (Fig. S7, ESI†).

Overall, CD studies confirmed the formation of ordered chiral ensembles of two-component systems (**APA** and dB_n) by way of mutual templating and chiral imprinting through double zipper assembly (Fig. 1).

These results prompted us to study the effect of pH, one of the key factors that influence hydrogen bonding (nucleobases) and electrostatic (sugar phosphate backbone) interactions of dB_n.[5] In the pH range of 2–11, a flat CD signal was observed for **APA** in the absence of dB_n. **APA** : dT_{10} (10 : 2) and **APA** : dT_{20} (20 : 2) showed very weak CD features corresponding to the perylene chromophore (400–600 nm) and dT_{10}/dT_{20} (250–300 nm) absorption regions in the acidic pH range of 2–4 (Fig. 2e and Fig. S8a, ESI†).[12] However, strong CD signals were observed for the perylene chromophore (400–600 nm) and dT_{10}/dT_{20} (250–300 nm) in the pH range of 7–11. CD spectra of **APA**:dA_{10}/dA_{20} displayed a flat signal in the 400–600 nm region under acidic conditions (pH = 2–4). Remarkably, at neutral pH **APA**:dA_{10}/dA_{20} exhibited strong positive CD signals in the 400–600 nm and 250–300 nm regions. The intensities of these signals were further enhanced by increasing the pH from 7 to 11 (Fig. 2f and Fig. S8b, ESI†).[12] Interestingly, **APA**:dA_{20} showed a positive CD signal while **APA**:dA_{10} did not show any appreciable CD signal in the adenine absorption region (250–300 nm) under acidic conditions (pH = 2–4). These pH-dependent transformations in the CD signatures of **APA**:dA_{10}/dA_{20} are mainly attributed to protonation of adenine. In acidic media (pH = 2–4), adenine (N^1) underwent protonation with the protonated N^1-H, triggering self-complementary base pairing [d(AH^+):d(AH^+)] through reverse Hoogsteen (H) hydrogen bonding.[7b] This facilitates the formation of homoduplexes (A-motifs) of dA_{10}/dA_{20}, which are further stabilized by electrostatic interactions with the phosphate backbone.[7b] It should be noted that a well-defined and characteristic CD signature for the self-complementary A-motif is observed with dA_n where $n \geq 12$.[7b] However, under neutral and basic conditions the unconventional A:A hydrogen bonding interaction driven by **APA** templating of dA_{10}/dA_{20} dominates to form hybrid DNA ensembles (Fig. 1).

Next, we recorded CD spectra of **APA** in the presence of dG_{10} and dC_{10} over a pH range of 2–11. Surprisingly, **APA** : dG_{10} (10 : 2) showed CD features similar to **APA** : dT_{10} (10 : 2), albeit only under neutral pH conditions (Fig. S9b, ESI†).[12] Stable unconventional hydrogen bonding-driven G–A pairing between **APA** and dG_{10} under neutral conditions led to the formation of [dG_{10}:(**APA**)$_{10}$:dG_{10}] ensembles.[8] The CD spectra of the **APA** and dC_{10} mixture (10 : 2) displayed a flat signal in the pH range of 7–11, as these conditions do not favor the formation of A–C base pairing. However, under acidic conditions (pH = 4) an intense positive CD signal at 294 nm and a negative CD-signal at 265 nm were observed. These are the characteristic CD features well-documented in the literature for *i-motifs* of dC_{10} under acidic conditions (Fig. S9a, ESI†).[12,14] Overall, pH ≥ 7 favored the mutual templating and chiral imprinting of **APA** and dB_n (B = T/A/G) through conventional and unconventional hydrogen bonding to form hybrid DNA ensembles of the type [dB_n:(**APA**)$_n$:dB_n].

In order to ascertain the thermal stability of helical ensembles of dB_n and **APA**, we carried out variable-temperature absorption and CD studies (Fig. S10 & S11, ESI†). Hybrid ensembles of purine-containing dB_n and **APA** exhibited high thermal stability as indicated by the melting temperatures (T_m) (Table 1). The thermal denaturation data revealed that all helical DNA ensembles of **APA** and dB_n were highly stable under ambient conditions. To visualize the structural morphology of hybrid helical DNA ensembles, we carried out atomic force microscopy (AFM) measurements on [dT_{20}:(**APA**)$_{20}$:dT_{20}] (A/T = 1 : 1) assembly structures. The AFM micrograph clearly showed formation of ordered left-handed helical assembly of [dT_{20}:(**APA**)$_{20}$:dT_{20}] (Fig. 3a and Fig. S12a, ESI†). The left-handed helical assembly structure is well-corroborated with the observed negative cotton effect in the CD spectrum of the [dT_{20}:(**APA**)$_{20}$:dT_{20}] ensemble (Fig. S7, ESI†). The AFM section profiles of [dT_{20}:(**APA**)$_{20}$:dT_{20}] structures revealed a typical helical pitch of ~22 nm along the *A*-axis (Fig. 3b) and a height (thickness) of 5 ± 0.5 nm along the *B*-axis (Fig. 3c). The observed thickness (5 ± 0.5 nm) is in agreement with the theoretically calculated value of 4.5 nm across (*B*-axis) hydrogen bonded **APA** and dT_{20} in [dT_{20}:(**APA**)$_{20}$:dT_{20}] (Fig. S12b, ESI†). Furthermore, the length of [dT_{20}:(**APA**)$_{20}$:dT_{20}] structures is in the range of 100–400 nm which is more than the individual ensemble (Fig. S12, ESI†). The observed longer helical assembly structures allowed us to

Table 1 Melting temperatures (T_m) of **APA** templated DNA ensembles

DNA complex	T_m (at pH = 7)	T_m (at pH = 9)
ds(A_{10} + T_{10})	21.1 °C	—
ds(G_{10} + C_{10})	62.0 °C	—
[dT_{10} + (**APA**)$_{10}$ + dT_{10}]	55.2 °C	60.1 °C
[dT_{20} + (**APA**)$_{20}$ + dT_{20}]	63.3 °C	64.1 °C
[dA_{10} + (**APA**)$_{10}$ + dA_{10}]	67.3 °C	65.7 °C
[dA_{20} + (**APA**)$_{20}$ + dA_{20}]	75.4 °C	65.7 °C
[dG_{10} + (**APA**)$_{10}$ + dG_{10}]	73.8 °C	—
[dG_{20} + (**APA**)$_{20}$ + dG_{20}]	78.3 °C	—

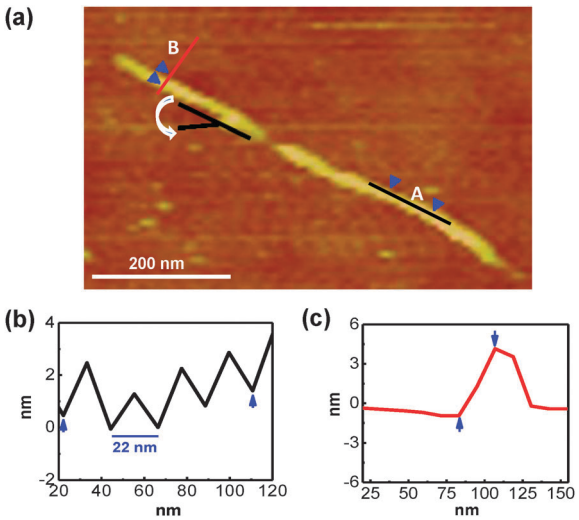

Fig. 3 (a) AFM image of left-handed helical DNA ensemble [dT_{20}–(**APA**)$_{20}$–dT_{20}]. (b) and (c) Section profiles of the DNA ensemble (a) along *A*- and *B*-axis. Helical pitch and height (thickness) of the DNA ensemble are found to be ~22 nm along the *A*-axis (b) and 5 nm along the *B*-axis (c) respectively. For clarity, section profiles corresponding to helical pitch and thickness are shown on different ensemble-structures. Inset: arrow shows the counter clockwise direction of the DNA ensemble to the symmetry axis.

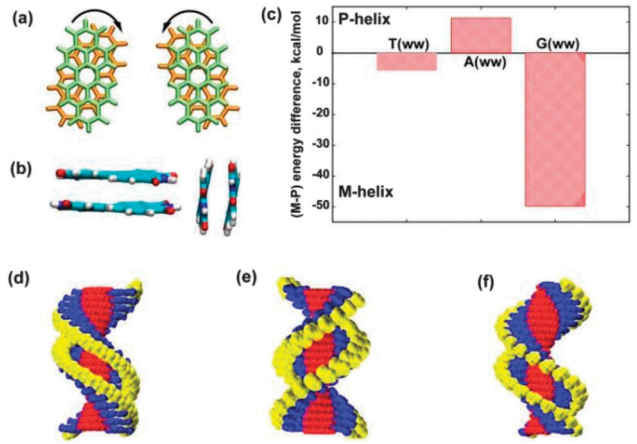

Fig. 4 Modeling PBI core of **APA** in dimer geometries. (a) Top view of the clock and anti-clockwise twisting in PBI dimers, (b) observed bent in the optimized PBI dimer structure and (c) difference between Boltzmann weighted averages of heat of formation values (in kcal mol^{-1}) of the left (M) and right (P) handed [dB_n–(**APA**)$_n$–dB_n] (B = A/T/G) helices. (d–f) Models of hybrid DNA ensembles [dT_{20}–(**APA**)$_{20}$–dT_{20}], [dA_{20}–(**APA**)$_{20}$–dA_{20}], and [dG_{20}–(**APA**)$_{20}$–dG_{20}], in their stable form.

consider end-to-end extension of individual ensembles through weak interactions which is very much anticipated on the surface. Overall, these studies proved the versatility of conventional and unconventional hydrogen bonding potential of adenine as the key factor for constructing stable helical hybrid DNA ensembles.

To understand the structure and energetics of the double zipper assembly, quantum mechanical (QM) calculations were performed on carefully chosen model systems, details of which are given in the ESI.†[12] The PBI dimer, optimized using the M06 and PM7 methods, yielded a non-planar structure (Fig. 4a & b). Several model systems for **APA** have been built appropriately including several conformations.[12] High level QM calculations at the RI-MP2 level of theory indicated that both A:A and A:G prefer W:W type base pairing over other possibilities (Fig. 1c & d). The relative energies of four model systems with two base pair steps for each of the M- and P-helical forms were calculated at the semi-empirical PM7 and the Boltzmann weighted differences are presented in Fig. 4c. The energies suggest that dT_n and dG_n prefer M-helical forms, whereas dA_n prefers to form the P-helix, which is in excellent agreement with the experimental observation discussed above. Based on these structures, a three-dimensional model for the most stable helical ensemble in each of the three cases was built and is given in Fig. 4d–f. A complex combination of several factors including unique conformational preferences of the backbone increased pitch, and solvent effects are proposed to yield such structures of the assemblies.

In conclusion, we demonstrated the versatility of conventional and unconventional hydrogen bonding ability of adenine in **APA** as a robust double zipper molecular template to construct hybrid DNA ensembles of random coiled deoxyoligonucleotides. The formation of ordered M- and P-helical DNA ensembles was achieved by distinctive base pairing (A–T, A–A and A–G) in the processes of mutual templating and chiral imprinting of **APA** and deoxyoligonucleotides at pH $\geq$ 7. These experimental results were further supported by AFM analysis and computational calculations. DNA-templated studies that have been reported so far probe the helical assembly of chromophores based on their characteristic CD signatures. In the present work, we showed mutual helical assembly of functional chromophores and oligonucleotides with corresponding characteristic CD signatures in their respective absorption regions for the formation of M- and P-helical DNA ensembles. The results reported here are likely to inspire the development of new hybrid DNA ensembles of functional molecules (organic chromophores with interesting optical, electronic and biological properties) and oligonucleotides for diverse applications. The properties and applications range from electronics to nanotechnology to biomedicine. The pH dependent hydrogen bonding ability of nucleobases in the DNA ensembles can be used as a tool for the development of stimuli responsive (pH-triggered) delivery systems for therapeutic small molecules and oligonucleotides.

We thank Prof. C. N. R. Rao FRS for constant support, JNCASR, the Department of Biotechnology (DBT) [BT/PR10263/NNT/28/711/2013 and BT/03/IYBA/2010], Govt. of India, New Delhi, for financial support and CSIR for SRF to NN and GS.

Notes and references

1 G. A. Jeffrey and W. Saenger, *Hydrogen Bonding in Biological Structures*, Springer, Berlin, 1991.
2 G. M. Whitsides and B. Grzvbowski, *Science*, 2002, **295**, 2418.
3 A. Hershey and M. Chase, *J. Gen. Physiol.*, 1952, **36**, 39.
4 J. Clayton and C. Dennis, *50 Years of DNA*, Nature Publishing Group, 20 Palgrave Macmillan, New York, 2003.
5 G. M. Blackburn, M. J. Gait, D. Loakes and D. M. Williams, *Nucleic Acids in Chemistry and Biology*, RSC Publishing, Cambridge, UK, 2006.
6 (*a*) K. C. Hannah and B. A. Armitage, *Acc. Chem. Res.*, 2004, **37**, 845; (*b*) R. Iwaura, F. J. M. Hoeben, M. Masuda, A. P. H. J. Schenning, E. W. Meijer and T. Shimizu, *J. Am. Chem. Soc.*, 2006, **128**, 13298; (*c*) J. G. Genereux and J. K. Barton, *Chem. Rev.*, 2010, **110**, 1642; (*d*) R. Iwaura, T. Iizawa, H. Minamikawa, M. Ohnishi-Kameyama and T. Shimizu, *Small*, 2010, **6**, 1131; (*e*) A. Ruiz-Carretero, P. G. A. Janssen, A. Kaeser and A. P. H. J. Schenning, *Chem. Commun.*, 2011, **47**, 4340; (*f*) M. Nakamura, T. Okaue, T. Takada and K. Yamana, *Chem. – Eur. J.*, 2012, **18**, 196; (*g*) A. Singer, S. Rapireddy, D. H. Ly and A. Mellar, *Nano Lett.*, 2012, **12**, 1722; (*h*) Y. N. Teo and E. T. Kool, *Chem. Rev.*, 2012, **112**, 4221.
7 (*a*) A. Rich, D. R. Davies, F. H. C. Crick and J. D. Watson, *J. Mol. Biol.*, 1961, **3**, 71; (*b*) S. Chakraborty, S. Sharma, P. K. Maiti and Y. Krishnan, *Nucleic Acids Res.*, 2009, **37**, 2810; (*c*) S. Verma, A. K. Mishra and J. Kumar, *Acc. Chem. Res.*, 2010, **43**, 79.
8 (*a*) T. Suda, Y. Mishima, H. Asakura and R. Kominami, *Nucleic Acids Res.*, 1995, **23**, 3771; (*b*) M. C. Shiber, E. H. Braswell, H. Klump and J. R. Fresco, *Nucleic Acids Res.*, 1996, **24**, 5004.
9 (*a*) F. Würthner, *Chem. Commun.*, 2004, 1564; (*b*) M. B. Avinash and T. Govindaraju, *Adv. Mater.*, 2012, **24**, 3905; (*c*) M. Li, C. Zhao, X. Yang, J. Ren and X. Qu, *Small*, 2013, **9**, 52.
10 (*a*) W. Wang, W. Wan, H. H. Zhou, S. Niu and A. D. Q. Li, *J. Am. Chem. Soc.*, 2003, **125**, 5248; (*b*) Y. Zheng, H. Long, G. C. Schatz and F. D. Lewis, *Chem. Commun.*, 2006, 3830.
11 (*a*) N. Narayanaswamy, M. B. Avinash and T. Govindaraju, *New J. Chem.*, 2013, **37**, 1302; (*b*) S. Manchineella, V. Prathyusha, U. D. Priyakumar and T. Govindaraju, *Chem. – Eur. J.*, 2013, **19**, 16615.
12 See ESI†.
13 K. Balakrishnan, A. Datar, R. Oitker, H. Chen, J. M. Zuo and L. Zang, *J. Am. Chem. Soc.*, 2005, **127**, 10496.
14 K. Gehring, J. L. Leroy and M. Guéron, *Nature*, 1993, **363**, 561.

